Aurora B kinase controls the targeting of the Astrin–SKAP complex to bioriented kinetochores

Jens C. Schmidt,[1,2] Tomomi Kiyomitsu,[1,2] Tetsuya Hori,[3,4,5] Chelsea B. Backer,[1,2] Tatsuo Fukagawa,[3,4,5] and Iain M. Cheeseman[1,2]

[1]Whitehead Institute for Biomedical Research, and [2]Department of Biology, Massachusetts Institute of Technology, Cambridge, MA 02142
[3]Department of Molecular Genetics, [4]National Institute of Genetics, and [5]The Graduate University for Advanced Studies (SOKENDAI), Mishima, Shizuoka 411-8540, Japan

During mitosis, kinetochores play multiple roles to generate interactions with microtubules, and direct chromosome congression, biorientation, error correction, and anaphase segregation. However, it is unclear what changes at the kinetochore facilitate these distinct activities. Here, we describe a complex of the spindle- and kinetochore-associated protein Astrin, the small kinetochore-associated protein (SKAP), and the dynein light chain LC8. Although most dynein-associated proteins localize to unaligned kinetochores in an Aurora B–dependent manner, Astrin, SKAP, and LC8 localization is antagonized by Aurora B such that they target exclusively to bioriented kinetochores. Astrin–SKAP-depleted cells fail to maintain proper chromosome alignment, resulting in a spindle assembly checkpoint–dependent mitotic delay. Consistent with a role in stabilizing bioriented attachments, Astrin and SKAP bind directly to microtubules and are required for CLASP localization to kinetochores. In total, our results suggest that tension-dependent Aurora B phosphorylation can act to control outer kinetochore composition to provide distinct activities to prometaphase and metaphase kinetochores.

Introduction

Proper chromosome segregation requires the macromolecular kinetochore to mediate interactions between chromosomal DNA and spindle microtubules (Cheeseman and Desai, 2008). During prometaphase, kinetochore–microtubule attachments are established that allow chromosomes to congress to the middle of the cell. In cases where erroneous interactions with the mitotic spindle occur, kinetochore–microtubule attachments must be corrected. During metaphase, biorientation is maintained and microtubules undergo rapid changes in dynamics, resulting in kinetochore oscillations. Finally, during anaphase A, kinetochores move toward the spindle poles along depolymerizing microtubules. At present, it is unclear what alters kinetochore function to achieve these distinct activities. In principle, this could occur by regulating the activity of stably associated kinetochore proteins, or by changing kinetochore composition.

One key regulator of kinetochore function that has been implicated in both controlling kinetochore activity and assembly state is Aurora B kinase. Aurora B functions to sense and correct aberrant kinetochore–microtubule interactions (Ruchaud et al., 2007). Because of a spatial separation from its substrates (Liu et al., 2009), Aurora B phosphorylation at the outer kinetochore is high on misaligned kinetochores that are not under tension, but is reduced at aligned kinetochores. Aurora B can directly modulate kinetochore–microtubule attachments by altering the activity of key kinetochore proteins, including the microtubule binding KNL-1/MIS-12 complex/NDC80 complex (KMN) network (Cheeseman et al., 2006; DeLuca et al., 2006; Welburn et al., 2010). Aurora B has also been suggested to play a role in kinetochore assembly. In *Xenopus laevis* extracts, Aurora B activity is required for outer kinetochore assembly (Emanuele et al., 2008). Although a similarly strong effect is not observed in human cells (Welburn et al., 2010), Aurora B activity promotes the localization of Shugoshin/MEI-S332 (Resnick et al., 2006), MCAK (Andrews et al., 2004; Lan et al., 2004), and Kif2b (Bakhoum et al., 2009b) to centromeres. In contrast, Aurora B

Correspondence to Iain M. Cheeseman: icheese@wi.mit.edu

Abbreviations used in this paper: ACA, anti-centromere antibody; SAC, spindle assembly checkpoint; SKAP, small kinetochore-associated protein; STLC, S-trityl-L-cysteine.

The Rockefeller University Press $30.00
J. Cell Biol. Vol. 191 No. 2 269–280
www.jcb.org/cgi/doi/10.1083/jcb.201006129

phosphorylation opposes the recruitment of its counteracting protein phosphatase PP1 to kinetochores (Liu et al., 2010).

Here, we describe a complex composed of the spindle and kinetochore proteins Astrin (Chang et al., 2001; Mack and Compton, 2001; Gruber et al., 2002; Thein et al., 2007) and small kinetochore-associated protein (SKAP; Fang et al., 2009). The Astrin–SKAP complex is recruited only to kinetochores that are aligned at the metaphase plate. We demonstrate that Astrin–SKAP localization is antagonized by Aurora B phosphorylation such that they are enriched at kinetochores when Aurora B activity is inhibited and reduced when additional Aurora B kinase is recruited to the outer kinetochore. Astrin and SKAP also associate with the dynein light chain LC8 and are required for proper LC8 localization to kinetochores. Astrin–SKAP depletion results in a Mad2-dependent mitotic delay, and prevents CLASP from localizing to kinetochores. In total, our results suggest that tension-dependent Aurora B phosphorylation functions directly or indirectly to control the composition of the outer kinetochore in a chromosome-specific manner to stabilize metaphase-aligned chromosomes and prepare for anaphase.

Results and discussion

SKAP localizes to the spindle and outer kinetochore

In our ongoing proteomic analysis of the vertebrate kinetochore, we identified C15orf23 as a protein weakly associated with known kinetochore components. C15orf23 was also recently identified as SKAP (Fang et al., 2009). SKAP localizes to spindle microtubules and spindle poles throughout mitosis, and to kinetochores from metaphase to telophase (Fig. 1, A and B). At kinetochores, SKAP localizes peripherally to Ndc80, which is consistent with it functioning at the outer kinetochore (Fig. 1 C). Similar to human SKAP, the *Gallus gallus* (chicken) homologue ggSKAP localizes to the spindle throughout mitosis, and to kinetochores in metaphase and anaphase, but not during prophase or prometaphase in DT40 cells (Fig. 1 D). These results demonstrate that SKAP is a conserved component of the vertebrate spindle and outer kinetochore.

SKAP and Astrin form a complex in vivo

To determine whether SKAP interacts with additional proteins, we conducted one step immunoprecipitations (IPs) from cells stably expressing GFP^{LAP}-SKAP or FLAG-ggSKAP. Mass spectrometry analysis of these purifications identified a complex of SKAP and the established spindle and kinetochore protein Astrin (also called SPAG5 or MAP126; Fig. 2, A and B; Chang et al., 2001; Mack and Compton, 2001; Gruber et al., 2002; Thein et al., 2007). Reciprocal purifications with GFP^{LAP}-Astrin isolated SKAP, confirming this association (Fig. 2, A and B). In addition to Astrin and SKAP, the only other proteins found in these purifications but not in controls were the dynein light chain LC8 (DYNLL1 and DYNLL2) and cytoplasmic dynein heavy chain (Fig. 2, A and B). Importantly, reciprocal purification of GFP^{LAP}-LC8 isolated Astrin in addition to the expected components of the dynein complex (Fig. 2 A). Previous studies identified Aurora A kinase and Glycogen synthase kinase 3β as Astrin-interacting proteins (Cheng et al., 2008; Du et al., 2008), but we did not detect either protein in our purifications.

Consistent with a direct interaction and with previous observations of Astrin localization (Mack and Compton, 2001; Thein et al., 2007; Manning et al., 2010), Astrin localized identically to SKAP throughout the cell cycle, including a preference for metaphase kinetochores relative to unaligned prometaphase kinetochores (Fig. 2 C; not depicted). Astrin and SKAP also displayed largely interdependent localization to spindles and kinetochores (Fig. 2 C), although small amounts of Astrin remain at kinetochores in SKAP-depleted cells. Both Astrin and SKAP were depleted by >90% after 48 h of treatment with the corresponding siRNAs, whereas the levels of the other complex component were subtly reduced (Fig. 2 D). In total, these results identified a complex of the spindle and kinetochore-associated proteins Astrin and SKAP.

SKAP and Astrin associate with microtubules directly

The localization of the Astrin–SKAP complex to spindle microtubules led us to test whether either protein associated with microtubules directly. In microtubule cosedimentation assays, we found that both full-length GST-SKAP and a C-terminal fragment of Astrin associated with microtubules (Fig. 2 E). In contrast, the C terminus of SKAP did not bind to microtubules. The dissociation constant for binding of GST-SKAP to microtubules is between 2 and 5 μM, which is slightly weaker than that of the Ndc80 complex under similar conditions (Cheeseman et al., 2006). These observations suggest that the Astrin–SKAP complex can associate with microtubules via domains in both SKAP and Astrin.

The Astrin–SKAP complex localizes preferentially to aligned chromosomes

We next sought to determine the relationship of the Astrin–SKAP complex to other established outer kinetochore components in both human and chicken cells. Depletion of KNL1 or the Ndc80 complex subunit Nuf2 prevented SKAP localization to kinetochores (Fig. 2 F and Fig. S1, A and B). In contrast, depletion of other established outer kinetochore components including Ska3, CENP-E, CENP-F, and CLASP1/2 codepletion did not completely prevent Astrin–SKAP localization to kinetochores (Fig. 2 F and Fig. S1 A). However, although these depletions had no effect on SKAP localization to kinetochores aligned at the metaphase plate, SKAP failed to localize to the misaligned chromosomes caused by each of these perturbations (Fig. 2 F, enlarged panels on the right). Because similar results are observed in multiple distinct depletions, this suggests that the Astrin–SKAP complex preferentially localizes to bioriented kinetochores.

Aurora B activity counteracts Astrin–SKAP localization to kinetochores

As kinetochores become bioriented, the tension that is applied to the sister kinetochores changes substantially (Maresca and Salmon, 2009; Uchida et al., 2009). This tension decreases phosphorylation of outer kinetochore substrates for Aurora B kinase such that levels are high on misaligned chromosomes relative to aligned chromosomes (Liu et al., 2009; Welburn et al., 2010).

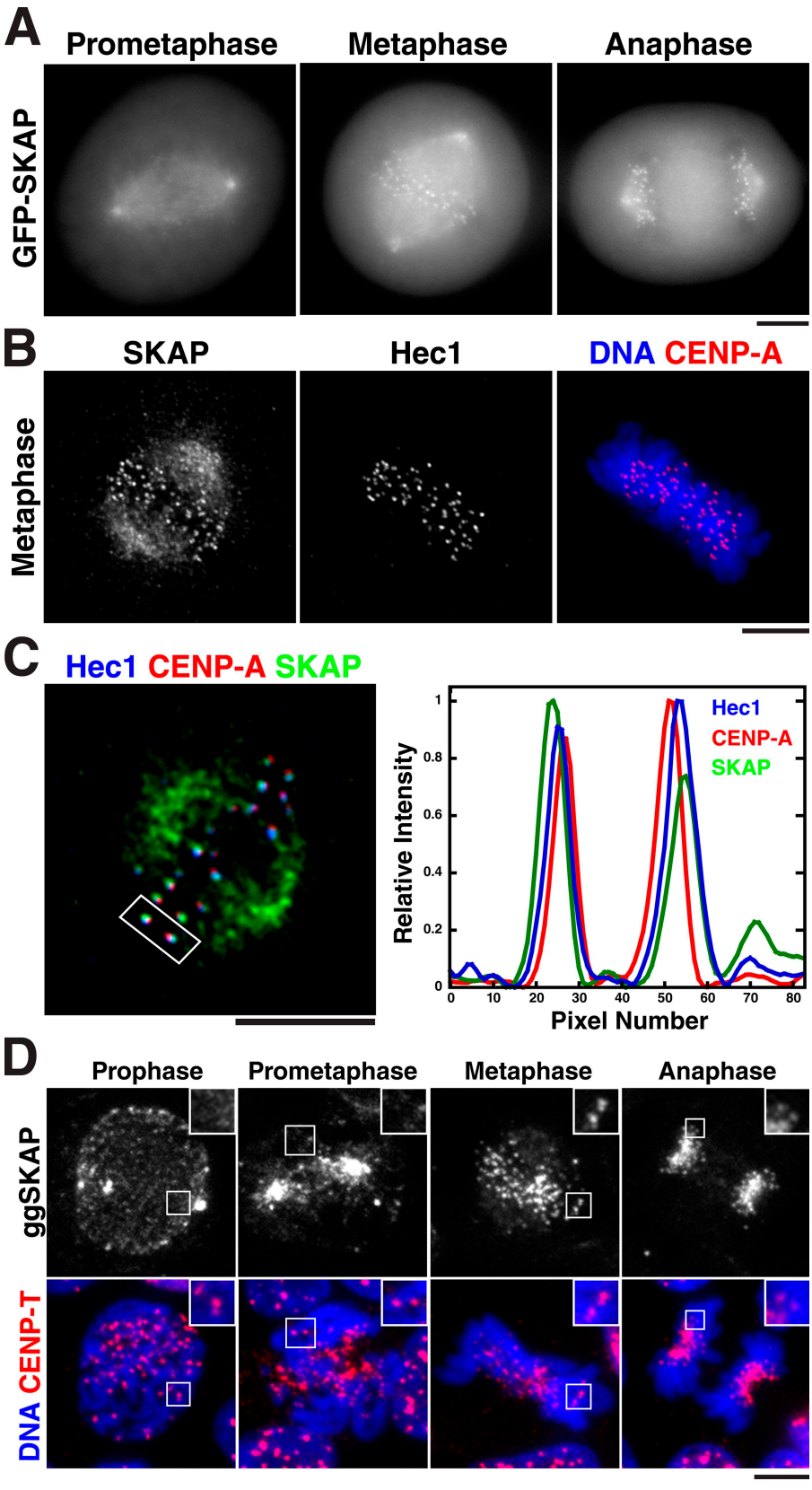

Figure 1. **SKAP localizes to the outer kinetochore during metaphase and anaphase.** (A) Images of different mitotic stages from a clonal human cell line stably expressing moderate amounts of GFP^{LAP}-SKAP. GFP-SKAP localizes to spindle microtubules throughout mitosis, and kinetochores during metaphase and anaphase. (B) Immunofluorescence showing the colocalization of SKAP and Hec1/Ndc80 with DNA (blue) and CENP-A (red). (C, left) Immunofluorescence image showing the colocalization of SKAP (green), Hec1 (blue), and CENP-A (red). (C, right) Graph showing a line scan from the boxed kinetochore pair showing the relative spatial distribution of SKAP, Hec1, and CENP-A. SKAP localizes slightly peripherally to Hec1 at the outer kinetochore. (D) Localization of chicken ggSKAP in DT40 cells. (D, top) SKAP alone. (D, bottom) Colocalization of DNA (blue) and CENP-T (red). Insets show enlarged views of the boxed regions. Bars, 5 µm.

Because SKAP and Astrin localize preferentially to kinetochores that are aligned at the metaphase plate, we sought to test the relationship between Aurora B activity and Astrin–SKAP localization.

We first analyzed the localization of the Astrin–SKAP complex relative to the level of Aurora B phosphorylation at a given kinetochore. In cells treated with low-dose nocodazole (10 ng/ml) to generate cells that contain both aligned (Fig. 3 A;

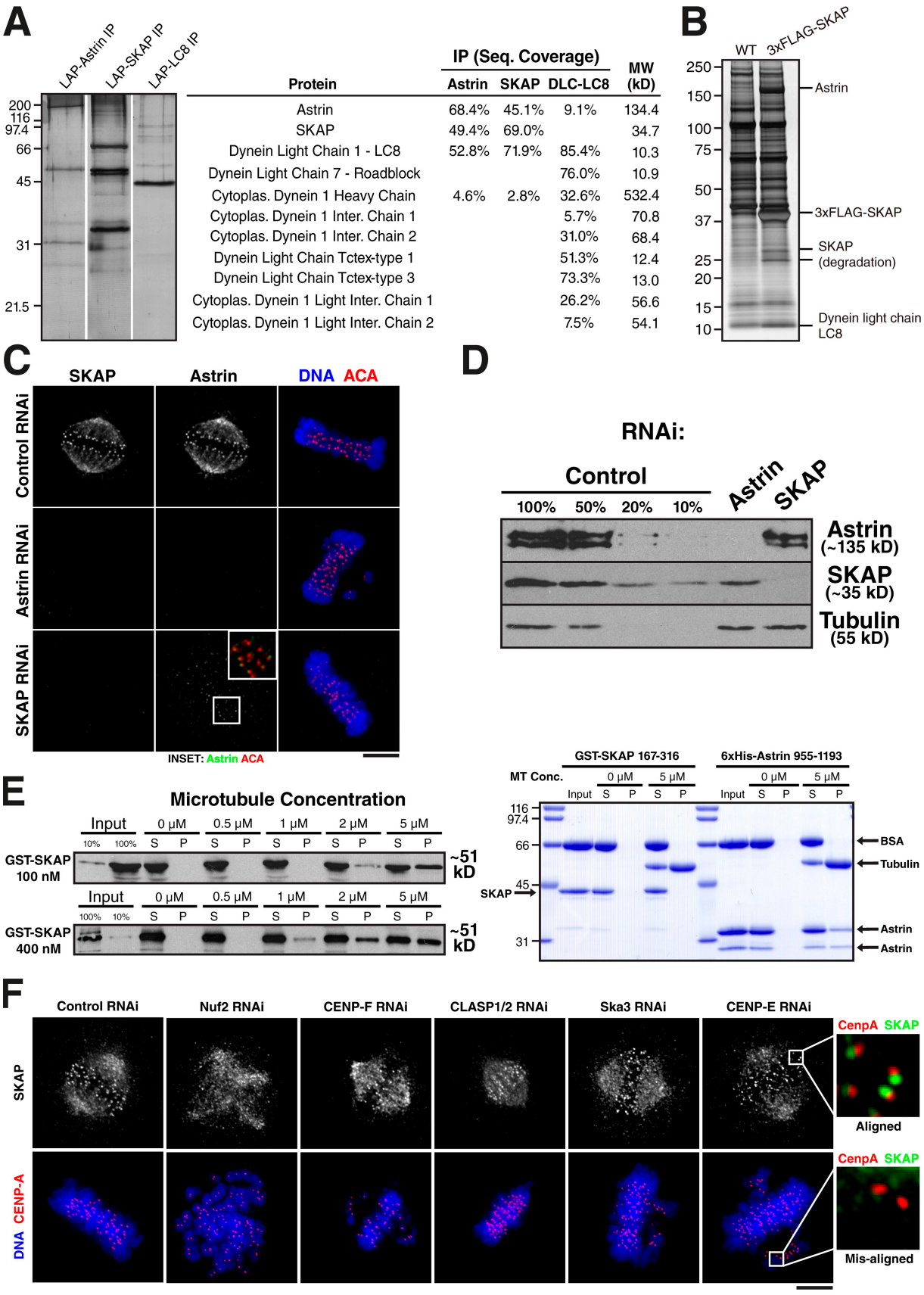

Figure 2. **SKAP and Astrin form a complex.** (A, left) Silver-stained gels showing a one-step IP of GFP^{LAP}-Astrin, GFP^{LAP}-SKAP, or GFP^{LAP}-LC8. (A, right) Data from the mass spectrometric analysis of the purifications indicating the percent sequence coverage from each IP. (B) Silver-stained gel showing the purification of FLAG-SKAP from chicken DT40 cells relative to controls. The indicated proteins were identified by excising them from a gel and analyzing

bottom arrow) and misaligned (top arrow) kinetochores, Aurora B phosphorylation, detected using antibodies that recognize an Aurora B phosphorylation site in Dsn1 (Welburn et al., 2010), was increased by 50% on the misaligned kinetochores (Fig. 3 A). In contrast, Astrin levels were reduced by >85% on the same misaligned kinetochores (Fig. 3 A). We observed microtubules apparently bound to these misaligned kinetochores (data not shown), which suggests that the localization of Astrin–SKAP is inversely proportional to Aurora B phosphorylation, not specifically the kinetochore attachment state.

To test the role of Aurora B phosphorylation in regulating Astrin–SKAP localization directly, we treated cells with the Aurora B inhibitor ZM447493. In ZM447493-treated cells, SKAP localizes to kinetochores that are syntelically oriented (Fig. 3 B, arrows), and thus are not under tension, which suggests that Aurora B activity normally counteracts Astrin–SKAP localization. Aurora B inhibition also promotes the localization of Astrin to misaligned kinetochores in U2OS cells (Manning et al., 2010). Next, we treated cells with the Eg5 inhibitor S-trityl-L-cysteine (STLC) which maintains kinetochore–microtubule attachments but reduces tension. STLC treatment increases Aurora B phosphorylation (Welburn et al., 2010) and reduces SKAP localization relative to aligned kinetochores in control cells (Fig. 3 B). However, cells treated with both STLC and ZM447493 showed significantly increased SKAP levels (Fig. 3 B), confirming that Aurora B activity has a negative effect on SKAP localization to kinetochores. Importantly, SKAP localization depends on both Aurora B activity and the presence of microtubules because treatment with the microtubule-depolymerizing drug nocodazole in either the presence or absence of ZM447493 prevented the localization of SKAP to kinetochores (Fig. 3 B).

To take a reciprocal approach to analyze the effect of Aurora B on Astrin–SKAP localization, we expressed a Mis12-INCENP-mCherry fusion, which has been shown to increase phosphorylation by recruiting additional Aurora B to the outer kinetochore (Liu et al., 2009). Expressing the Mis12-INCENP-mCherry fusion reduced the levels of GFP-SKAP at kinetochores by more than twofold (Fig. 3 C), even though these kinetochores remain apparently bioriented. In contrast, a Mis12-INCENP(TAA)-mCherry mutant, which binds to but does not activate Aurora B (Sessa et al., 2005), had no effect on the levels of GFP^{LAP}-SKAP at kinetochores (Fig. 3 C). To take an alternate approach to increase Aurora B phosphorylation, we eliminated the ability of KNL1 to target PP1, the counteracting phosphatase for Aurora B, to kinetochores (Liu et al., 2010). For these experiments, we depleted endogenous KNL1 and replaced this with a protein lacking the N terminus. Cells lacking the PP1-targeting domain in KNL1 displayed greatly reduced Astrin at kinetochores (Fig. S1 C), but showed normal localization of the Mis12 complex subunit Dsn1 (unpublished data). However, treatment with the Aurora B inhibitor ZM447493 restored Astrin localization to kinetochores, demonstrating that Astrin is specifically sensitive to the level of Aurora B phosphorylation at kinetochores. In each case described above, inhibiting or increasing Aurora B phosphorylation produced similar results for Astrin and SKAP localization (unpublished data).

We conclude that local Aurora B kinase activity has a negative effect on Astrin–SKAP localization to kinetochores. The levels of both proteins are reduced when Aurora B activity at the outer kinetochore is high, and increased when Aurora B activity is reduced, causing them to localize exclusively to bioriented kinetochores.

Depletion of the Astrin–SKAP complex results in a checkpoint-dependent mitotic delay in human cells

To determine the role of the Astrin–SKAP complex in chromosome segregation, we conducted time-lapse imaging of HeLa cells expressing YFP-histone H2B. Chromosome congression in SKAP- or Astrin-depleted cells proceeded with kinetics that were similar, but slightly slower than control cells (Fig. 4 A). However, the time that chromosomes remained aligned at the metaphase plate before transitioning to anaphase was significantly increased in SKAP-depleted cells (Fig. 4, A and B). During this extended delay, we often observed individual chromosomes losing alignment and moving to the poles before realigning (Fig. 4 A, arrows). In rare cases, the chromosomes would decondense without undergoing anaphase. This phenotype is more severe than that previously reported for SKAP depletion (Fang et al., 2009), but is similar to the phenotype described for Astrin depletion (Thein et al., 2007).

To determine whether the prolonged mitotic delay observed after SKAP depletion is dependent on the spindle assembly checkpoint (SAC), we simultaneously depleted SKAP and the checkpoint component Mad2. Codepletion of SKAP and Mad2 allowed cells to proceed quickly through mitosis, indicating that the observed mitotic delay is dependent on the SAC (Fig. 4, A and B). Although a subset of chromosomes align at the metaphase plate in Astrin- and SKAP-depleted cells, we found that BubR1 is highly enriched on the misaligned chromosomes generated by Astrin depletion (Fig. 4 C), which suggests that the SAC arrest is caused by the failure to maintain chromosome alignment. This contrasts with a previous study that proposed that the delay caused by SKAP depletion is downstream of the SAC (Fang et al., 2009).

them by mass spectrometry. (C) Astrin and SKAP show interdependent localization. Immunofluorescence images showing Astrin and SKAP localization in control cells, or cells depleted for Astrin or SKAP relative to DNA (blue) and kinetochores (ACA; red). (D) Western blot probed for anti-Astrin (top), anti-SKAP (middle), and anti-Tubulin (bottom) antibodies showing the efficiency of SKAP and Astrin depletion. (E) SKAP and Astrin bind to microtubules in vitro. (E, left) Western blot probed with anti-SKAP antibodies showing the cosedimentation of GST-SKAP with microtubules. (E, right) Coomassie stained gel showing the cosedimentation of a fragment of Astrin (955–1193) with microtubules, but the inability of GST-SKAP C-terminal fragment to bind to microtubules. (F) SKAP localizes exclusively to aligned kinetochores. Immunofluorescence images showing SKAP localization in cells treated with control siRNAs or siRNAs against Nuf2, CENP-E, CENP-F, CLASP1 and CLASP2, or Ska3. DNA is shown in blue, and CENP-A staining is shown in red. SKAP localization requires Nuf2, but does not absolutely require the other proteins. However, in these cases, SKAP localizes only to aligned kinetochores, but not to misaligned kinetochores (enlarged views). Also see Fig. S1. Molecular mass standards are indicated in kilodaltons next to the gel blots. Bars, 5 µm.

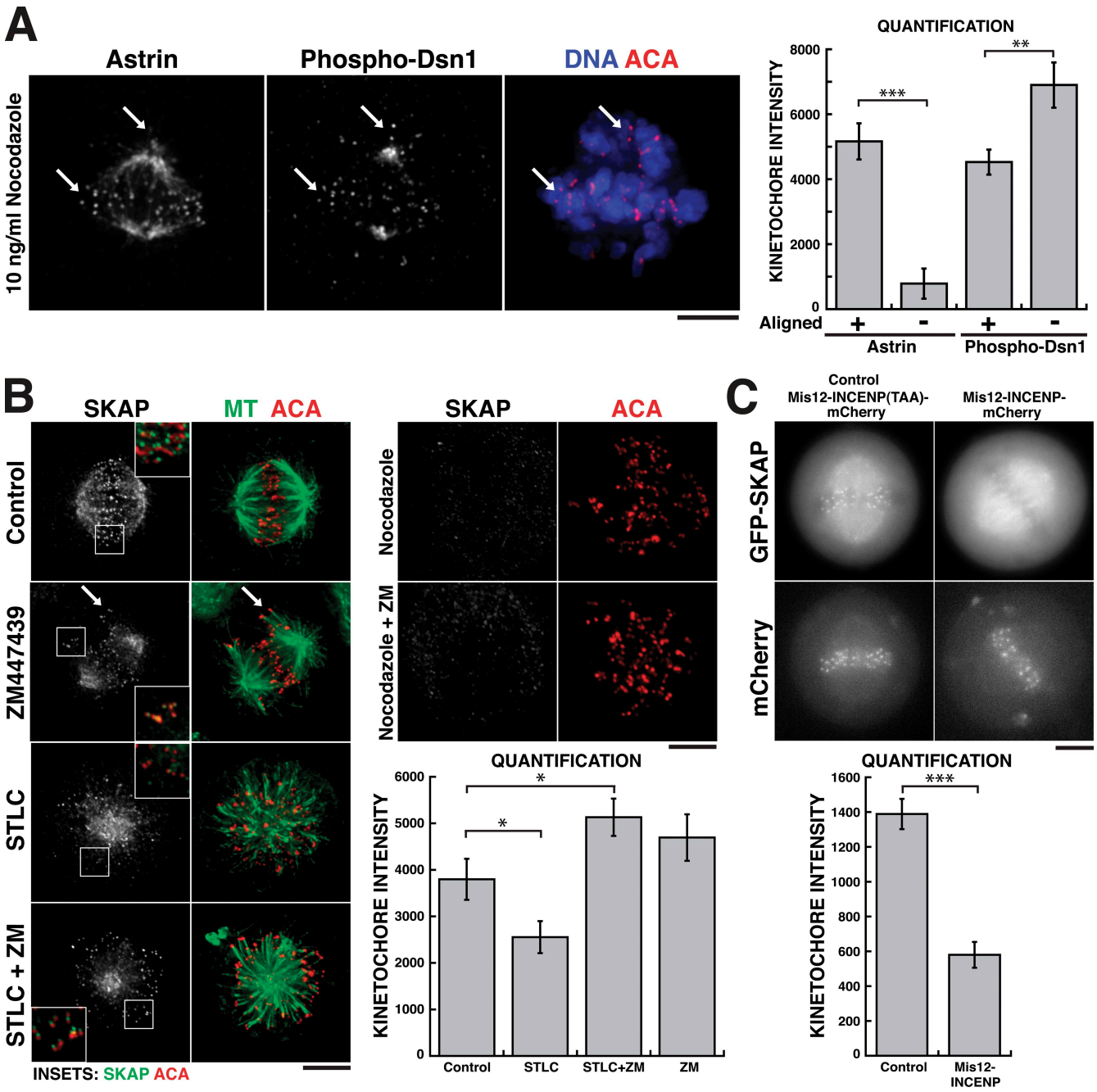

Figure 3. **SKAP localization to kinetochores is counteracted by local Aurora B activity.** (A) Astrin localization is inversely proportional to the level of Aurora B phosphorylation at a specific kinetochore. (A, left) Immunofluorescence images showing Astrin localization relative to phospho-Dsn1, and to DNA (blue) and kinetochores (ACA; red), in a cell treated with low-dose nocodazole (10 ng/ml) to generate both aligned and misaligned kinetochores (indicated by arrows). (A, right) Quantification of Astrin and phospho-Dsn1 localization at aligned (n = 5 cells, 59 kinetochores) and misaligned (n = 5 cells, 48 kinetochores) kinetochores. **, a significant difference with $P < 0.01$; ***, $P < 0.001$. Bars, 5 µm. (B) Immunofluorescence images showing SKAP localization relative to microtubules and ACA in either control cells (n = 7 cells, 108 kinetochores), cells treated individually the Aurora B inhibitor ZM447439 (n = 6 cells, 90 kinetochores), the Eg5 inhibitor STLC (n = 8 cells, 165 kinetochores), or the microtubule-depolymerizing drug nocodazole, or combinations of STLC and ZM447439 (n = 10 cells, 170 kinetochores) or nocodazole and ZM447439. Quantification of the kinetochore intensity of SKAP (bottom right) indicates that inhibiting Aurora B activity increases the localization of SKAP to kinetochores. *, statistically significant differences with $P < 0.05$. Insets show enlarged views of the boxed regions. (C) Images from live cells showing the colocalization of GFP-SKAP with either Mis12-INCENP-mCherry (n = 7 cells, 92 kinetochores) or Mis12-INCENP-mCherry fusion in which the residues in INCENP that activate Aurora B are mutated to TAA as a control (n = 7 cells, 92 kinetochores). The Mis12-INCENP fusion increases Aurora B activity at the outer kinetochore (Liu et al., 2009). Quantification (bottom) indicates that the Mis12-INCENP fusion decreases SKAP localization to kinetochores. Error bars indicate SEM. ***, a significant difference with $P < 0.001$.

To determine whether this checkpoint-dependent arrest after SKAP or Astrin depletion is caused by defective kinetochore–microtubule attachments, we measured the interkinetochore distances. For these experiments, we monitored chromosomes that aligned at the metaphase plate. The presence of bioriented attachments under tension in control cells caused the separation of sister kinetochores by ~1.2 µm relative to ~0.65 µm in nocodazole-treated cells (Fig. 4 D; not depicted). Depletion of

proteins that compromise kinetochore–microtubule attachments, such as the Mis12 complex subunit Dsn1, resulted in a reduction of interkinetochore stretch by ~30% (Fig. 4 D). In contrast, Astrin- and SKAP-depleted cells show a 25% increase in this stretched distance (Fig. 4 D), which indicates that, if anything, interkinetochore tension is increased. Thus, Astrin and SKAP display a checkpoint-dependent arrest despite their ability to initially biorient sister chromatids, align chromosomes at the metaphase plate, and develop interkinetochore tension.

The Astrin–SKAP complex is required to target CLASP to kinetochores

Both Astrin and SKAP were recently identified in purifications with the microtubule plus end tracking protein CLASP (Maffini et al., 2009). Because we found that codepletion of CLASP1 and CLASP2 did not affect the localization of SKAP to aligned kinetochores (Fig. 2 F), we sought to determine whether the Astrin–SKAP complex affects CLASP targeting. Strikingly, we found that after depletion of Astrin, CLASP1 failed to localize to kinetochores (Fig. 4 E). Astrin depletion has been shown to destabilize spindle microtubules (Bakhoum et al., 2009a; Manning et al., 2010), a finding consistent with the idea that delocalization of CLASP, which affects microtubule dynamics (Maiato et al., 2003), may contribute to the defects observed in Astrin-depleted cells.

SKAP deletion is viable, but displays some mitotic defects in chicken DT40 cells

To determine the role of SKAP in chicken, we generated a deletion of SKAP in DT40 cells (Fig. S2). SKAP-deficient cells are viable, with a growth rate similar to that of wild-type DT40 cells, and display normal localization of kinetochore proteins such as the Ndc80 complex subunit Nuf2 (Fig. 4 F). SKAP knockout cells show relatively normal numbers of the different mitotic stages, but have a small increase in cells with multipolar spindles (Fig. 4 F). SKAP knockout cells also show increased mitotic defects upon removal of the microtubule-depolymerizing drug nocodazole relative to control cells (unpublished data). Thus, although the temporal localization and physical associations of SKAP are conserved in chickens, SKAP displays an increased functional requirement for chromosome segregation during an unperturbed cell division in human cells. A similar difference is observed for other outer kinetochore components, with Ska3 and ZW10 being essential for proper chromosome segregation in human cells but dispensable for viability in DT40 cells (unpublished data).

Aurora B differentially affects the targeting of distinct dynein subunits to kinetochores

Astrin and SKAP associate with the dynein light chain LC8, as well as with small amounts of the cytoplasmic dynein heavy chain (Fig. 2 A). LC8 has been implicated in the retrograde transport of dynein substrates, although it remains unclear whether LC8 mediates interactions with dynein cargo molecules or plays a different role (Puthalakath et al., 1999; Williams et al., 2007). The interaction with LC8 is surprising, as previous work on dynein suggested that it displays very different temporal localization from Astrin–SKAP to kinetochores (Pfarr et al., 1990; Steuer et al., 1990). Indeed, we found that the dynactin subunit Arp1 and the dynein light chain Tctex (DYNLT3) showed localization to kinetochores during prometaphase, but not metaphase and anaphase (Fig. 5 A). In contrast, LC8 localized to metaphase and anaphase kinetochores, but not prometaphase kinetochores (Fig. 5 A). Thus, LC8 displays identical temporal localization to Astrin and SKAP during mitosis, including a preference for aligned kinetochores.

Astrin–SKAP complex localization to the outer kinetochore is strongly influenced by Aurora B activity (Fig. 3). Based on the close connection between Astrin–SKAP and the dynein-associated protein LC8, we sought to determine the dependence of other dynein-interacting proteins on Aurora B phosphorylation. In contrast to Astrin–SKAP, we found that Aurora B activity is required to promote Tctex and Arp1 localization, as ZM447493 treatment eliminated their localization from kinetochores in STLC-treated cells (Fig. 5 B). However, although expression of the Mis12-INCENP fusion prevented LC8 localization to kinetochores (Fig. 5 C), this did not allow Tctex and Arp1 to localize to aligned kinetochores (Fig. 5, D and E). This suggests either that both Aurora B and microtubule attachments affect Tctex and Arp1 localization, or that the additional Aurora B phosphorylation provided by the Mis12-INCENP fusion is not sufficient to target them to kinetochores. In contrast, LC8 behaves identically to Astrin and SKAP, with its localization inhibited by local Aurora B activity (Fig. 5, B and C). Importantly, the localization of LC8 to both the spindle and kinetochore during mitosis requires Astrin (Fig. 5 F). In contrast, dynein depletion did not alter Astrin–SKAP localization to aligned kinetochores (Fig. S1 D), and codepletion of the two LC8 isoforms present in human cells does not affect SKAP localization or perturb mitotic progression (Fig. S3 and not depicted).

Whether the Astrin–SKAP complex recruits a subpopulation of dynein to metaphase kinetochores through LC8 remains an open question. Importantly, we did find the cytoplasmic dynein motor associated with Astrin and SKAP in our purifications (Fig. 2 A). However, if present, the pool of dynein at the metaphase kinetochores would only transiently interact with the Astrin–SKAP complex before moving toward the spindle pole via kinetochore microtubules. In total, this work suggests that there are two populations of dynein-interacting proteins: those whose kinetochore localization is promoted by Aurora B activity, and a second group including LC8 and Astrin–SKAP whose kinetochore localization is antagonized by Aurora B.

Aurora B phosphorylation provides a switch for outer kinetochore composition

When sister chromatids are correctly aligned and under tension, the reduction of Aurora B phosphorylation at the outer kinetochore (Liu et al., 2009; Welburn et al., 2010) allows the Astrin–SKAP complex to be recruited to kinetochores (Fig. 3). This may occur through the changes in the phosphorylation state of a kinetochore-bound Astrin–SKAP-binding protein,

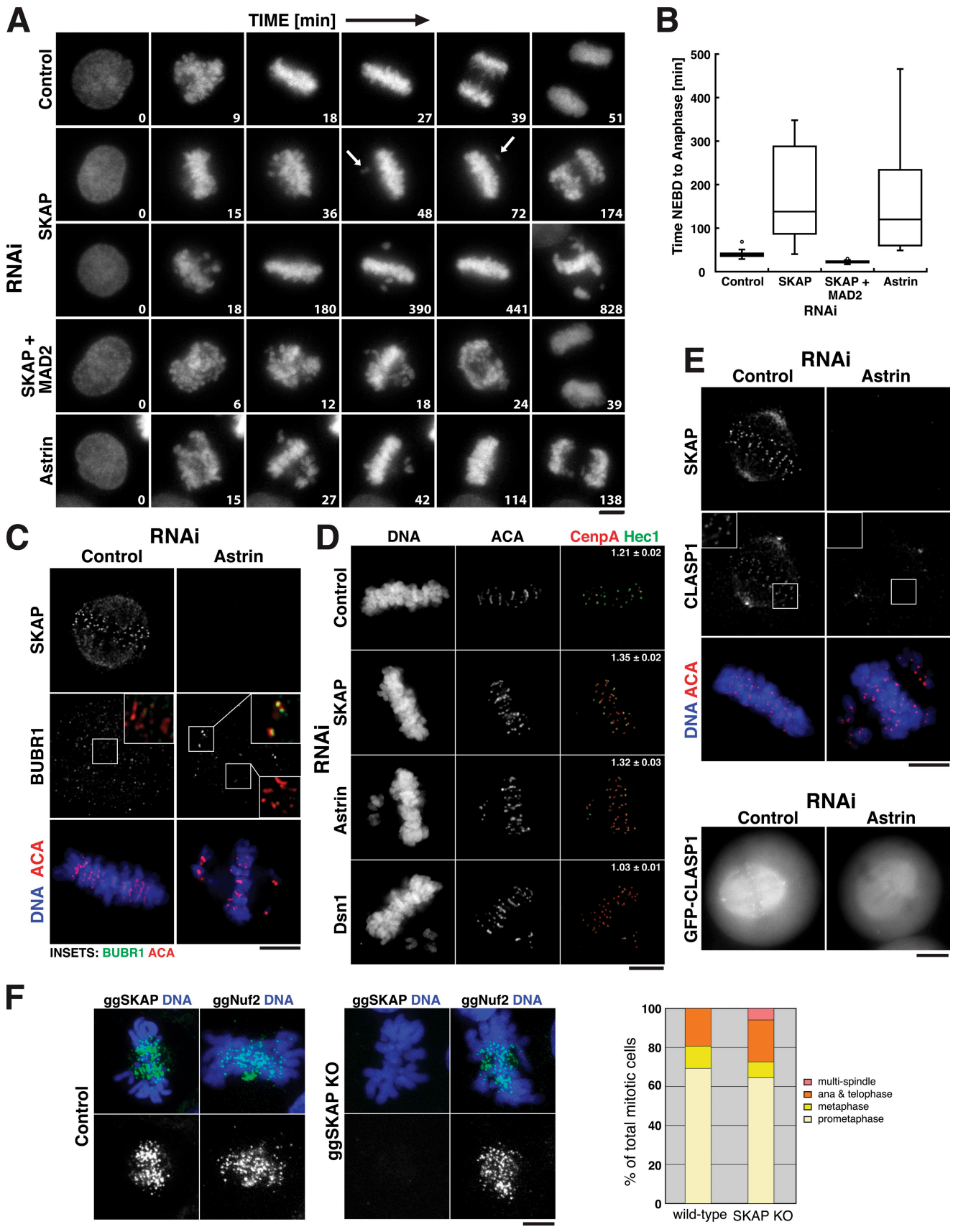

Figure 4. **Astrin and SKAP depletion causes a checkpoint-dependent mitotic arrest.** (A) Selected images from time-lapse movies of HeLa cells expressing YFP-H2B in either control cells, SKAP-depleted cells, Astrin-depleted cells, or SKAP and Mad2 codepleted cells. Numbers in each image indicate the relative time in minutes. Also see Videos 1–5. Bar, 5 µm. (B) Box plot showing the quantification of the time from nuclear envelope breakdown (NEBD) to anaphase

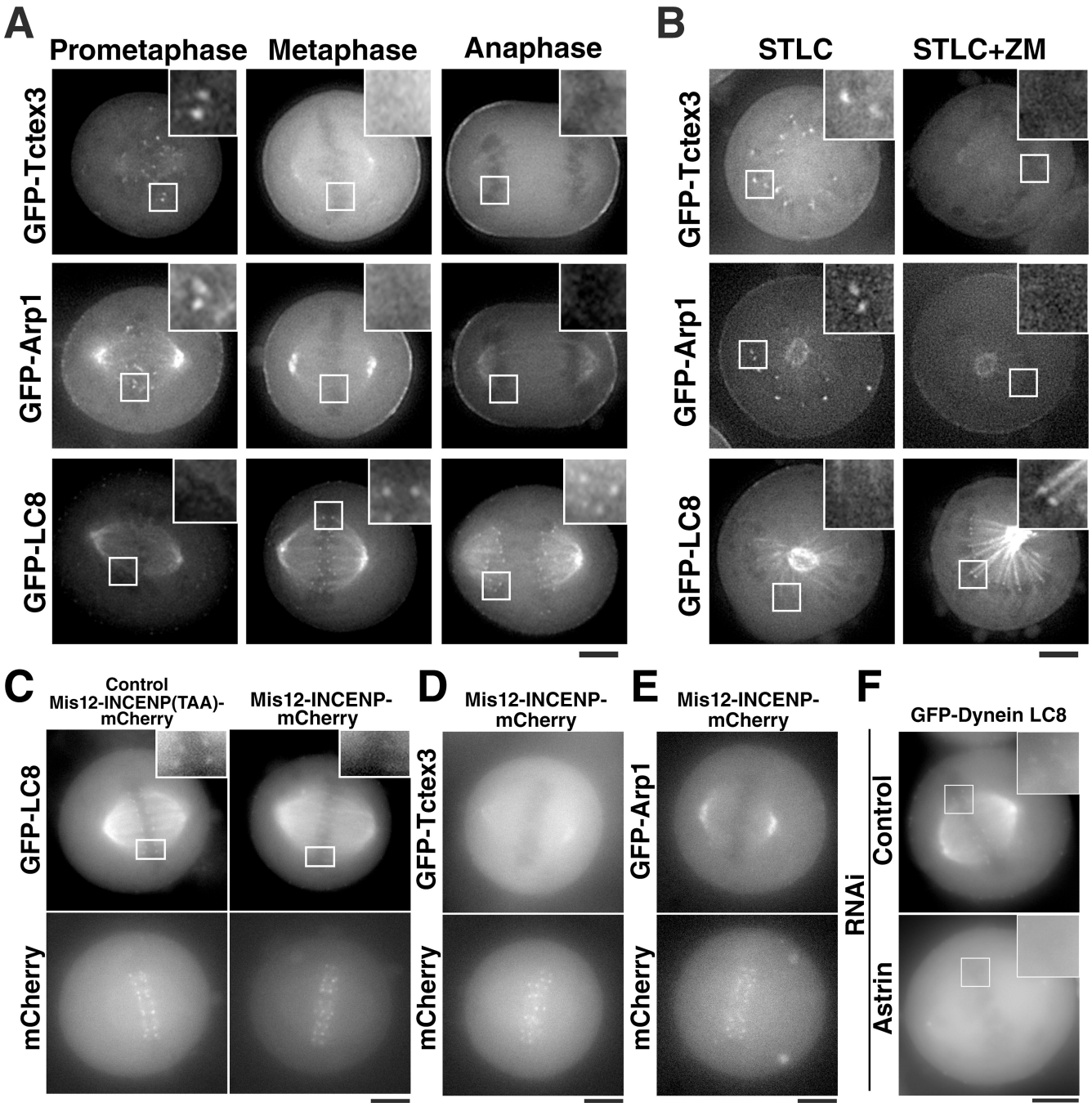

Figure 5. **Aurora B provides a switch in the targeting of different dynein subunits to kinetochores.** (A) Images showing the localization of the dynein light chains GFP^{LAP}-Tctex3 and GFP^{LAP}-LC8, or the dynactin subunit GFP^{LAP}-Arp1 in different stages of mitosis. (B) Images showing the localization of GFP^{LAP}-Tctex3, GFP^{LAP}-LC8, or GFP^{LAP}-Arp1 in STLC-treated cells, or STLC plus ZM447493–treated cells. (C–E) Images showing the localization of GFP^{LAP}-Tctex3, GFP^{LAP}-LC8, or GFP^{LAP}-Arp1 and either Mis12-INCENP(TAA)-mCherry (control) or Mis12-INCENP-mCherry–transfected cells as indicated. (F) Images showing the localization of GFP-LC8 in either control or Astrin-depleted cells. Insets show enlarged views of the boxed regions. Bars, 5 µm.

onset indicating the median time, quartiles, and minimum and maximum values. (C) BubR1 is enriched on misaligned kinetochores in Astrin-depleted cells. Immunofluorescence images showing ACA (red), BubR1 (green), DNA, and SKAP in control and Astrin-depleted cells. (D) Astrin and SKAP depletion increase interkinetochore distance. Immunofluorescence images showing CENP-A (red), Hec1 (green), ACA, and DNA in either control (n = 6 cells, 151 kinetochores), Astrin- (n = 3 cells, 30 kinetochores, $P < 0.01$), SKAP- (n = 10 cells, 160 kinetochores, $P < 0.0001$), or Dsn1-depleted cells (n = 6 cells, 130 kinetochores, $P < 0.0001$). Numbers indicate the mean interkinetochore distance based on CENP-A ± SEM. (E) Astrin is required for CLASP localization to kinetochores. (E, top) Immunofluorescence images showing ACA (red), DNA (blue), CLASP1, and SKAP in either control or Astrin-depleted cells. Insets show enlarged views of the boxed regions. (E, bottom) GFP-CLASP1 localization in live control or Astrin-depleted cells. (F) ggSKAP deletion in chicken DT40 cells does not alter Nuf2 localization. Immunofluorescence images showing ggSKAP or ggNuf2 localization (in green in merge) and DNA (blue) in either control DT40 cells or SKAP knockout cells. See Fig. S2 for the generation of the SKAP knockout cell line. (F) Graph showing the percentage of different mitotic states in either control DT40 cells or ggSKAP knockout cells. Bars, 5 µm.

or changes in the stability and number of kinetochore-bound microtubules that facilitate Astrin–SKAP recruitment. In either case, this provides a mechanism to recruit and exclude proteins from the outer kinetochore depending on the state of attachment and tension, with Aurora B phosphorylation molecularly distinguishing the two states. Such a mechanism would allow protein activities to be specifically recruited to correctly bioriented kinetochores, possibly to stabilize metaphase attachments or execute anaphase. Importantly, the Astrin–SKAP complex is only present at bioriented kinetochores, but not kinetochores with attachment defects, which suggests that this complex does not function in the error correction process downstream of Aurora B. Instead, this raises the intriguing possibility that Aurora B phosphorylation generates a switch that molecularly distinguishes the composition of prometaphase and metaphase kinetochores in a chromosome-autonomous fashion.

Materials and methods

Cell culture and siRNA transfection

cDNAs were obtained as IMAGE clones. Stable clonal cells lines expressing GFP^{LAP} fusions were generated in HeLa cells as described previously (Cheeseman et al., 2004). We obtained HeLa cells expressing YFP-CENP-A (Kops et al., 2005) and YFP-H2B. Cells were maintained in DME supplemented with 10% FBS, penicillin/streptomycin, and L-glutamine (Invitrogen) at 37°C in a humidified atmosphere with 5% CO_2. RNAi experiments were conducted as described previously (Kline et al., 2006). siRNAs against Astrin (5′-UCCCGACAACUCACAGAGAAA-3′; Thein et al., 2007), SKAP (5′-GAAAGAGUCCGAUUCCUAG-3′; Thermo Fisher Scientific), LC8-1/DYNLL1 (5′-GUUCAAAUCUGGUUAAAAG-3′, 5′-GAAGGACAUUGCGGCUCAU-3′, 5′-GUACUAGUUUGUCGUGGUU-3′, and 5′-CAGCCUAAAUUCCAAAUAC-3′; Thermo Fisher Scientific), LC8-2/DYNLL2 (5′-GGAAGGCAGUGAUCAAGAA-3′, 5′-GACAAGAAAUAUAACCCUA-3′, 5′-CCAUGGAGAAGUACAAUAU-3′, and 5′-CAAAGCACUUCAUCUAUUU-3′; Thermo Fisher Scientific), Nuf2 (5′-AAGCAUGCCGUGAAACGUAUA-3′; DeLuca et al., 2002), CENP-E (5′-AAGGCUACAAUGGUACUAUA-3′; Kapoor et al., 2006), CENP-F (5′-GAGAAGACCCCAAGUCAUC-3′; Johnson et al., 2004), a pool of four siRNAs targeting Ska3 (Welburn et al., 2009), Mad2 (5′-UACGGACUCACCUUGCUUG-3′; Martin-Lluesma et al., 2002), CLASP1 (5′-GGAUGAUUUACAAGACUGG-3′; Mimori-Kiyosue et al., 2005), CLASP2 (5′-GACAUACAUGGGUCUUAGA-3′; Mimori-Kiyosue et al., 2005), and a nontargeting control were obtained from Thermo Fisher Scientific. For codepletions, individual siRNAs were first validated by combining these with an equal volume of nontargeting control siRNAs to ensure that they were still effective under these conditions.

Immunofluorescence and microscopy

Immunofluorescence in human cells was conducted as described previously (Kline et al., 2006). For immunofluorescence against microtubules, DM1α (Sigma-Aldrich) was used at 1:500. For visualization of kinetochore proteins, we used phospho-Dsn1 (Welburn et al., 2010), mouse anti-HEC1 (9G3; Abcam), mouse anti-Astrin (a gift from M.-S. Chang, Institute of Biochemical Sciences, National Taiwan University, Taipei, Taiwan; Yang et al., 2006), mouse anti-CLASP1 (a gift from H. Maiato, Institute for Molecular and Cell Biology [IBMC], Porto, Portugal), mouse anti-BubR1 (8G1; Abcam), rabbit anti-LC8-1 (Abcam), and human anti-centromere antibodies (ACAs; Antibodies, Inc.). An affinity-purified rabbit polyclonal antibody was generated against full-length SKAP as described previously (Desai et al., 2003). Cy2-, Cy3-, and Cy5-conjugated secondary antibodies (Jackson ImmunoResearch Laboratories, Inc.) were used at 1:100. DNA was visualized using 10 µg/ml Hoechst.

For drug treatment, HeLa cells were incubated for 2–3 h with drugs at the following concentrations: 10 µM STLC, 0.2 µg/ml nocodazole, and 2 µM ZM447439. Mis12-INCENP-mCherry and Mis12-INCENP(TAA)-mCherry plasmids (Liu et al., 2009) were a gift from S. Lens (University Medical Center Utrecht, Utrecht, Netherlands). To quantitate fluorescence intensity, individual kinetochores were selected from projections (chosen blindly based on colocalization with a separate stable kinetochore marker), and the integrated intensity was determined after subtracting the background fluorescence measured from adjacent regions of the cell using MetaMorph software (Roper Industries). Fluorescence levels at kinetochores were normalized with respect to control cells. At least 5–10 cells were examined for each condition and antibody.

Images were acquired on a deconvolution microscope (DeltaVision Core; Applied Precision) equipped with a CoolSnap HQ2 charge-coupled device camera. 30–40 z sections were acquired at 0.2-µm steps using a 100×, 1.3 NA Olympus U-Plan Apochromat objective lens with 1 × 1 binning. Images were deconvolved using the DeltaVision software. Images shown represent maximal intensity projections. Equivalent exposure conditions and scaling was used between controls and RNAi-depleted cells.

Analysis of SKAP in chicken DT40 cells

DT40 cells were cultured at 38°C in Dulbecco's modified medium supplemented with 10% fetal calf serum, 1% chicken serum, β-mercaptoethanol, penicillin, and streptomycin, and transfected as described previously (Fukagawa et al., 2001). The SKAP-targeted constructs were generated to disrupt four exons of the ggSKAP gene (Fig. S2). After transfection, drug-resistant colonies were isolated, and Southern blot hybridization analysis was performed to identify clones in which the targeted integrations occurred correctly.

Immunofluorescent staining of DT40 cells was performed as described previously (Hori et al., 2008). Affinity-purified rabbit polyclonal antibodies were used against recombinant chicken Nuf2 (Hori et al., 2003) and SKAP (this paper). Chromosomes and nuclei were counterstained with DAPI at 0.2 µg/ml in Vectashield Antifade (Vector Laboratories). For the immunofluorescence images, 30–40 z sections were collected at 0.2-µm intervals with a cooled EM charge-coupled device camera (Quantem; Roper Industries) mounted on an inverted microscope (Olympus IX71) with a 100× objective together with a filter wheel. Subsequent analysis and processing of images were performed using Metamorph software.

Protein purification and biochemical assays

GFP^{LAP} tagged Astrin and SKAP were isolated from HeLa cells as described previously (Cheeseman and Desai, 2005). Purified proteins were identified by mass spectrometry using an LTQ XL Ion trap mass spectrometer (Thermo Fisher Scientific) using MudPIT and SEQUEST software as described previously (Washburn et al., 2001).

For the expression and purification of the recombinant proteins, a GST fusion with full-length SKAP was generated in pGEX-6P-1, and 6xHis-Astrin (955–1193) was generated in pRSETa. Proteins were purified using glutathione agarose (Sigma-Aldrich) or Ni-NTA agarose (QIAGEN) according to the manufacturer's instructions, then desalted into 50 mM Hepes, pH 7.5, 200 mM KCl, 1 mM EDTA, and 1 mM DTT (HEK200). Microtubule binding assays using the purified proteins were conducted as described previously (Cheeseman et al., 2006) using equal volumes of microtubules in BRB80 and test protein in HEK200.

Online supplemental material

Fig. S1 shows an extended analysis of the requirements for Astrin and SKAP localization to kinetochores including several additional depletion conditions. Fig. S2 shows the strategy and validation to generate the chicken DT40 cell SKAP knockout. Fig. S3 shows an analysis of the contribution of LC8 to chromosome segregation and SKAP localization. Video 1 shows a time-lapse movie of mitosis and chromosome segregation in control cells. Videos 2 and 3 show mitosis in SKAP-depleted cells. Video 4 shows mitosis in Astrin-depleted cells. Video 5 shows mitosis in a cell co-depleted for SKAP and Mad2. Online supplemental material is available at http://www.jcb.org/cgi/content/full/jcb.201006129/DC1.

We thank Duane Compton for sharing results before publication, Mau-Sun Chang for his generosity in sharing the monoclonal Astrin antibody, Susanne Lens for the Mis12-INCENP plasmids, Helder Maiato for helpful discussions and sharing the anti-CLASP1 antibody, and Michael Lampson, Angelika Amon, and members of the Cheeseman laboratory for helpful discussions and critical reading of the manuscript.

This work was supported by awards to I.M. Cheeseman from the Smith Family Foundation, the Massachusetts Life Sciences Center, and the Searle Scholars Program; a grant to I.M. Cheeseman from the National Institute Of General Medical Sciences (GM088313); and Grants-in-Aid for Scientific Research from the Ministry of Education, Culture, Science and Technology (MEXT) of Japan to T. Fukagawa. I.M. Cheeseman is a Thomas D. and Virginia W. Cabot Career Development Professor of Biology.

Submitted: 22 June 2010
Accepted: 14 September 2010

References

Andrews, P.D., Y. Ovechkina, N. Morrice, M. Wagenbach, K. Duncan, L. Wordeman, and J.R. Swedlow. 2004. Aurora B regulates MCAK at the mitotic centromere. *Dev. Cell.* 6:253–268. doi:10.1016/S1534-5807(04)00025-5

Bakhoum, S.F., G. Genovese, and D.A. Compton. 2009a. Deviant kinetochore microtubule dynamics underlie chromosomal instability. *Curr. Biol.* 19:1937–1942. doi:10.1016/j.cub.2009.09.055

Bakhoum, S.F., S.L. Thompson, A.L. Manning, and D.A. Compton. 2009b. Genome stability is ensured by temporal control of kinetochore-microtubule dynamics. *Nat. Cell Biol.* 11:27–35. doi:10.1038/ncb1809

Chang, M.S., C.J. Huang, M.L. Chen, S.T. Chen, C.C. Fan, J.M. Chu, W.C. Lin, and Y.C. Yang. 2001. Cloning and characterization of hMAP126, a new member of mitotic spindle-associated proteins. *Biochem. Biophys. Res. Commun.* 287:116–121. doi:10.1006/bbrc.2001.5554

Cheeseman, I.M., and A. Desai. 2005. A combined approach for the localization and tandem affinity purification of protein complexes from metazoans. *Sci. STKE.* 2005:pl1. doi:10.1126/stke.2662005pl1

Cheeseman, I.M., and A. Desai. 2008. Molecular architecture of the kinetochore-microtubule interface. *Nat. Rev. Mol. Cell Biol.* 9:33–46. doi:10.1038/nrm2310

Cheeseman, I.M., S. Niessen, S. Anderson, F. Hyndman, J.R. Yates III, K. Oegema, and A. Desai. 2004. A conserved protein network controls assembly of the outer kinetochore and its ability to sustain tension. *Genes Dev.* 18:2255–2268. doi:10.1101/gad.1234104

Cheeseman, I.M., J.S. Chappie, E.M. Wilson-Kubalek, and A. Desai. 2006. The conserved KMN network constitutes the core microtubule-binding site of the kinetochore. *Cell.* 127:983–997. doi:10.1016/j.cell.2006.09.039

Cheng, T.S., Y.L. Hsiao, C.C. Lin, C.T. Yu, C.M. Hsu, M.S. Chang, C.I. Lee, C.Y. Huang, S.L. Howng, and Y.R. Hong. 2008. Glycogen synthase kinase 3beta interacts with and phosphorylates the spindle-associated protein astrin. *J. Biol. Chem.* 283:2454–2464. doi:10.1074/jbc.M706794200

DeLuca, J.G., B. Moree, J.M. Hickey, J.V. Kilmartin, and E.D. Salmon. 2002. hNuf2 inhibition blocks stable kinetochore-microtubule attachment and induces mitotic cell death in HeLa cells. *J. Cell Biol.* 159:549–555. doi:10.1083/jcb.200208159

DeLuca, J.G., W.E. Gall, C. Ciferri, D. Cimini, A. Musacchio, and E.D. Salmon. 2006. Kinetochore microtubule dynamics and attachment stability are regulated by Hec1. *Cell.* 127:969–982. doi:10.1016/j.cell.2006.09.047

Desai, A., S. Rybina, T. Müller-Reichert, A. Shevchenko, A. Shevchenko, A. Hyman, and K. Oegema. 2003. KNL-1 directs assembly of the microtubule-binding interface of the kinetochore in *C. elegans. Genes Dev.* 17:2421–2435. doi:10.1101/gad.1126303

Du, J., S. Jablonski, T.J. Yen, and G.J. Hannon. 2008. Astrin regulates Aurora-A localization. *Biochem. Biophys. Res. Commun.* 370:213–219. doi:10.1016/j.bbrc.2008.03.072

Emanuele, M.J., W. Lan, M. Jwa, S.A. Miller, C.S. Chan, and P.T. Stukenberg. 2008. Aurora B kinase and protein phosphatase 1 have opposing roles in modulating kinetochore assembly. *J. Cell Biol.* 181:241–254. doi:10.1083/jcb.200710019

Fang, L., A. Seki, and G. Fang. 2009. SKAP associates with kinetochores and promotes the metaphase-to-anaphase transition. *Cell Cycle.* 8:2819–2827.

Fukagawa, T., Y. Mikami, A. Nishihashi, V. Regnier, T. Haraguchi, Y. Hiraoka, N. Sugata, K. Todokoro, W. Brown, and T. Ikemura. 2001. CENP-H, a constitutive centromere component, is required for centromere targeting of CENP-C in vertebrate cells. *EMBO J.* 20:4603–4617. doi:10.1093/emboj/20.16.4603

Gruber, J., J. Harborth, J. Schnabel, K. Weber, and M. Hatzfeld. 2002. The mitotic-spindle-associated protein astrin is essential for progression through mitosis. *J. Cell Sci.* 115:4053–4059. doi:10.1242/jcs.00088

Hori, T., T. Haraguchi, Y. Hiraoka, H. Kimura, and T. Fukagawa. 2003. Dynamic behavior of Nuf2-Hec1 complex that localizes to the centrosome and centromere and is essential for mitotic progression in vertebrate cells. *J. Cell Sci.* 116:3347–3362. doi:10.1242/jcs.00645

Hori, T., M. Amano, A. Suzuki, C.B. Backer, J.P. Welburn, Y. Dong, B.F. McEwen, W.-H. Shang, E. Suzuki, K. Okawa, et al. 2008. CCAN makes multiple contacts with centromeric DNA to provide distinct pathways to the outer kinetochore. *Cell.* 135:1039–1052. doi:10.1016/j.cell.2008.10.019

Johnson, V.L., M.I. Scott, S.V. Holt, D. Hussein, and S.S. Taylor. 2004. Bub1 is required for kinetochore localization of BubR1, Cenp-E, Cenp-F and Mad2, and chromosome congression. *J. Cell Sci.* 117:1577–1589. doi:10.1242/jcs.01006

Kapoor, T.M., M.A. Lampson, P. Hergert, L. Cameron, D. Cimini, E.D. Salmon, B.F. McEwen, and A. Khodjakov. 2006. Chromosomes can congress to the metaphase plate before biorientation. *Science.* 311:388–391. doi:10.1126/science.1122142

Kline, S.L., I.M. Cheeseman, T. Hori, T. Fukagawa, and A. Desai. 2006. The human Mis12 complex is required for kinetochore assembly and proper chromosome segregation. *J. Cell Biol.* 173:9–17. doi:10.1083/jcb.200509158

Kops, G.J., Y. Kim, B.A. Weaver, Y. Mao, I. McLeod, J.R. Yates III, M. Tagaya, and D.W. Cleveland. 2005. ZW10 links mitotic checkpoint signaling to the structural kinetochore. *J. Cell Biol.* 169:49–60. doi:10.1083/jcb.200411118

Lan, W., X. Zhang, S.L. Kline-Smith, S.E. Rosasco, G.A. Barrett-Wilt, J. Shabanowitz, D.F. Hunt, C.E. Walczak, and P.T. Stukenberg. 2004. Aurora B phosphorylates centromeric MCAK and regulates its localization and microtubule depolymerization activity. *Curr. Biol.* 14:273–286.

Liu, D., G. Vader, M.J. Vromans, M.A. Lampson, and S.M. Lens. 2009. Sensing chromosome bi-orientation by spatial separation of aurora B kinase from kinetochore substrates. *Science.* 323:1350–1353. doi:10.1126/science.1167000

Liu, D., M. Vleugel, C.B. Backer, T. Hori, T. Fukagawa, I.M. Cheeseman, and M.A. Lampson. 2010. Regulated targeting of protein phosphatase 1 to the outer kinetochore by KNL1 opposes Aurora B kinase. *J. Cell Biol.* 188:809–820. doi:10.1083/jcb.201001006

Mack, G.J., and D.A. Compton. 2001. Analysis of mitotic microtubule-associated proteins using mass spectrometry identifies astrin, a spindle-associated protein. *Proc. Natl. Acad. Sci. USA.* 98:14434–14439. doi:10.1073/pnas.261371298

Maffini, S., A.R. Maia, A.L. Manning, Z. Maliga, A.L. Pereira, M. Junqueira, A. Shevchenko, A. Hyman, J.R. Yates III, N. Galjart, et al. 2009. Motor-independent targeting of CLASPs to kinetochores by CENP-E promotes microtubule turnover and poleward flux. *Curr. Biol.* 19:1566–1572. doi:10.1016/j.cub.2009.07.059

Maiato, H., E.A. Fairley, C.L. Rieder, J.R. Swedlow, C.E. Sunkel, and W.C. Earnshaw. 2003. Human CLASP1 is an outer kinetochore component that regulates spindle microtubule dynamics. *Cell.* 113:891–904. doi:10.1016/S0092-8674(03)00465-3

Manning, A.L., S.F. Bakhoum, S. Maffini, C. Correia-Melo, H. Maiato, and D.A. Compton. 2010. CLASP1, astrin and Kif2b form a molecular switch that regulates kinetochore-microtubule dynamics to promote mitotic progression and fidelity. *EMBO J.* In press.

Maresca, T.J., and E.D. Salmon. 2009. Intrakinetochore stretch is associated with changes in kinetochore phosphorylation and spindle assembly checkpoint activity. *J. Cell Biol.* 184:373–381. doi:10.1083/jcb.200808130

Martin-Lluesma, S., V.M. Stucke, and E.A. Nigg. 2002. Role of Hec1 in spindle checkpoint signaling and kinetochore recruitment of Mad1/Mad2. *Science.* 297:2267–2270. doi:10.1126/science.1075596

Mimori-Kiyosue, Y., I. Grigoriev, G. Lansbergen, H. Sasaki, C. Matsui, F. Severin, N. Galjart, F. Grosveld, I. Vorobjev, S. Tsukita, and A. Akhmanova. 2005. CLASP1 and CLASP2 bind to EB1 and regulate microtubule plus-end dynamics at the cell cortex. *J. Cell Biol.* 168:141–153. doi:10.1083/jcb.200405094

Pfarr, C.M., M. Coue, P.M. Grissom, T.S. Hays, M.E. Porter, and J.R. McIntosh. 1990. Cytoplasmic dynein is localized to kinetochores during mitosis. *Nature.* 345:263–265. doi:10.1038/345263a0

Puthalakath, H., D.C. Huang, L.A. O'Reilly, S.M. King, and A. Strasser. 1999. The proapoptotic activity of the Bcl-2 family member Bim is regulated by interaction with the dynein motor complex. *Mol. Cell.* 3:287–296. doi:10.1016/S1097-2765(00)80456-6

Resnick, T.D., D.L. Satinover, F. MacIsaac, P.T. Stukenberg, W.C. Earnshaw, T.L. Orr-Weaver, and M. Carmena. 2006. INCENP and Aurora B promote meiotic sister chromatid cohesion through localization of the Shugoshin MEI-S332 in *Drosophila. Dev. Cell.* 11:57–68. doi:10.1016/j.devcel.2006.04.021

Ruchaud, S., M. Carmena, and W.C. Earnshaw. 2007. Chromosomal passengers: conducting cell division. *Nat. Rev. Mol. Cell Biol.* 8:798–812. doi:10.1038/nrm2257

Sessa, F., M. Mapelli, C. Ciferri, C. Tarricone, L.B. Areces, T.R. Schneider, P.T. Stukenberg, and A. Musacchio. 2005. Mechanism of Aurora B activation by INCENP and inhibition by hesperadin. *Mol. Cell.* 18:379–391. doi:10.1016/j.molcel.2005.03.031

Steuer, E.R., L. Wordeman, T.A. Schroer, and M.P. Sheetz. 1990. Localization of cytoplasmic dynein to mitotic spindles and kinetochores. *Nature.* 345:266–268. doi:10.1038/345266a0

Thein, K.H., J. Kleylein-Sohn, E.A. Nigg, and U. Gruneberg. 2007. Astrin is required for the maintenance of sister chromatid cohesion and centrosome integrity. *J. Cell Biol.* 178:345–354. doi:10.1083/jcb.200701163

Uchida, K.S., K. Takagaki, K. Kumada, Y. Hirayama, T. Noda, and T. Hirota. 2009. Kinetochore stretching inactivates the spindle assembly checkpoint. *J. Cell Biol.* 184:383–390. doi:10.1083/jcb.200811028

Washburn, M.P., D. Wolters, and J.R. Yates III. 2001. Large-scale analysis of the yeast proteome by multidimensional protein identification technology. *Nat. Biotechnol.* 19:242–247. doi:10.1038/85686

Welburn, J.P., E.L. Grishchuk, C.B. Backer, E.M. Wilson-Kubalek, J.R. Yates III, and I.M. Cheeseman. 2009. The human kinetochore Ska1 complex facilitates microtubule depolymerization-coupled motility. *Dev. Cell.* 16:374–385. doi:10.1016/j.devcel.2009.01.011

Welburn, J.P.I., M. Vleugel, D. Liu, J.R. Yates III, M.A. Lampson, T. Fukagawa, and I.M. Cheeseman. 2010. Aurora B phosphorylates spatially distinct targets to differentially regulate the kinetochore-microtubule interface. *Mol. Cell.* 38:383–392. doi:10.1016/j.molcel.2010.02.034

Williams, J.C., P.L. Roulhac, A.G. Roy, R.B. Vallee, M.C. Fitzgerald, and W.A. Hendrickson. 2007. Structural and thermodynamic characterization of a cytoplasmic dynein light chain-intermediate chain complex. *Proc. Natl. Acad. Sci. USA.* 104:10028–10033. doi:10.1073/pnas.0703614104

Yang, Y.C., Y.T. Hsu, C.C. Wu, H.T. Chen, and M.S. Chang. 2006. Silencing of astrin induces the p53-dependent apoptosis by suppression of HPV18 E6 expression and sensitizes cells to paclitaxel treatment in HeLa cells. *Biochem. Biophys. Res. Commun.* 343:428–434. doi:10.1016/j.bbrc.2006.02.166